

**Search for pair production of doubly-charged Higgs bosons
in the $H^{++}H^{--} \rightarrow \mu^+\mu^+\mu^-\mu^-$ final state at D0**

V.M. Abazov³⁶, B. Abbott⁷⁵, M. Abolins⁶⁵, B.S. Acharya²⁹, M. Adams⁵¹, T. Adams⁴⁹, E. Aguilo⁶, S.H. Ahn³¹, M. Ahsan⁵⁹, G.D. Alexeev³⁶, G. Alkhazov⁴⁰, A. Alton^{64,a}, G. Alverson⁶³, G.A. Alves², M. Anastasoie³⁵, L.S. Ancu³⁵, T. Andeen⁵³, S. Anderson⁴⁵, B. Andrieu¹⁷, M.S. Anzelc⁵³, M. Aoki⁵⁰, Y. Arnoud¹⁴, M. Arov⁶⁰, M. Arthaud¹⁸, A. Askew⁴⁹, B. Åsman⁴¹, A.C.S. Assis Jesus³, O. Atramentov⁴⁹, C. Avila⁸, C. Ay²⁴, F. Badaud¹³, A. Baden⁶¹, L. Bagby⁵⁰, B. Baldin⁵⁰, D.V. Bandurin⁵⁹, P. Banerjee²⁹, S. Banerjee²⁹, E. Barberis⁶³, A.-F. Barfuss¹⁵, P. Bargassa⁸⁰, P. Baringer⁵⁸, J. Barreto², J.F. Bartlett⁵⁰, U. Bassler¹⁸, D. Bauer⁴³, S. Beale⁶, A. Bean⁵⁸, M. Begalli³, M. Begel⁷³, C. Belanger-Champagne⁴¹, L. Bellantoni⁵⁰, A. Bellavance⁵⁰, J.A. Benitez⁶⁵, S.B. Beri²⁷, G. Bernardi¹⁷, R. Bernhard²³, I. Bertram⁴², M. Besançon¹⁸, R. Beuselinck⁴³, V.A. Bezzubov³⁹, P.C. Bhat⁵⁰, V. Bhatnagar²⁷, C. Biscarat²⁰, G. Blazey⁵², F. Blekman⁴³, S. Blessing⁴⁹, D. Bloch¹⁹, K. Bloom⁶⁷, A. Boehnlein⁵⁰, D. Boline⁶², T.A. Bolton⁵⁹, G. Borisso⁴², T. Bose⁷⁷, A. Brandt⁷⁸, R. Brock⁶⁵, G. Brooijmans⁷⁰, A. Bross⁵⁰, D. Brown⁸¹, N.J. Buchanan⁴⁹, D. Buchholz⁵³, M. Buehler⁸¹, V. Buescher²², V. Bunichev³⁸, S. Burdin^{42,b}, S. Burke⁴⁵, T.H. Burnett⁸², C.P. Buszello⁴³, J.M. Butler⁶², P. Calfayan²⁵, S. Calvet¹⁶, J. Cammin⁷¹, W. Carvalho³, B.C.K. Casey⁵⁰, H. Castilla-Valdez³³, S. Chakrabarti¹⁸, D. Chakraborty⁵², K. Chan⁶, K.M. Chan⁵⁵, A. Chandra⁴⁸, F. Charles^{19,‡}, E. Cheu⁴⁵, F. Chevallier¹⁴, D.K. Cho⁶², S. Choi³², B. Choudhary²⁸, L. Christofek⁷⁷, T. Christoudias⁴³, S. Cihangir⁵⁰, D. Claes⁶⁷, Y. Coadou⁶, M. Cooke⁸⁰, W.E. Cooper⁵⁰, M. Corcoran⁸⁰, F. Couderc¹⁸, M.-C. Cousinou¹⁵, S. Crépe-Renaudin¹⁴, D. Cutts⁷⁷, M. Cwiok³⁰, H. da Motta², A. Das⁴⁵, G. Davies⁴³, K. De⁷⁸, S.J. de Jong³⁵, E. De La Cruz-Burelo⁶⁴, C. De Oliveira Martins³, J.D. Degenhardt⁶⁴, F. Déliot¹⁸, M. Demarteau⁵⁰, R. Demina⁷¹, D. Denisov⁵⁰, S.P. Denisov³⁹, S. Desai⁵⁰, H.T. Diehl⁵⁰, M. Diesburg⁵⁰, A. Dominguez⁶⁷, H. Dong⁷², L.V. Dudko³⁸, L. Duflot¹⁶, S.R. Dugad²⁹, D. Duggan⁴⁹, A. Duperrin¹⁵, J. Dyer⁶⁵, A. Dyshkant⁵², M. Eads⁶⁷, D. Edmunds⁶⁵, J. Ellison⁴⁸, V.D. Elvira⁵⁰, Y. Enari⁷⁷, S. Eno⁶¹, P. Ermolov³⁸, H. Evans⁵⁴, A. Evdokimov⁷³, V.N. Evdokimov³⁹, A.V. Ferapontov⁵⁹, T. Ferbel⁷¹, F. Fiedler²⁴, F. Filthaut³⁵, W. Fisher⁵⁰, H.E. Fisk⁵⁰, M. Fortner⁵², H. Fox⁴², S. Fu⁵⁰, S. Fuess⁵⁰, T. Gadfort⁷⁰, C.F. Galea³⁵, E. Gallas⁵⁰, C. Garcia⁷¹, A. Garcia-Bellido⁸², V. Gavrilov³⁷, P. Gay¹³, W. Geist¹⁹, D. Gelé¹⁹, C.E. Gerber⁵¹, Y. Gershtein⁴⁹, D. Gillberg⁶, G. Ginther⁷¹, N. Gollub⁴¹, B. Gómez⁸, A. Goussiou⁸², P.D. Grannis⁷², H. Greenlee⁵⁰, Z.D. Greenwood⁶⁰, E.M. Gregores⁴, G. Grenier²⁰, Ph. Gris¹³, J.-F. Grivaz¹⁶, A. Grohsjean²⁵, S. Grünendahl⁵⁰, M.W. Grünewald³⁰, F. Guo⁷², J. Guo⁷², G. Gutierrez⁵⁰, P. Gutierrez⁷⁵, A. Haas⁷⁰, N.J. Hadley⁶¹, P. Haefner²⁵, S. Hagopian⁴⁹, J. Haley⁶⁸, I. Hall⁶⁵, R.E. Hall⁴⁷, L. Han⁷, K. Harder⁴⁴, A. Harel⁷¹, R. Harrington⁶³, J.M. Hauptman⁵⁷, R. Hauser⁶⁵, J. Hays⁴³, T. Hebbeker²¹, D. Hedin⁵², J.G. Hegeman³⁴, J.M. Heinmiller⁵¹, A.P. Heinson⁴⁸, U. Heintz⁶², C. Hensel⁵⁸, K. Herner⁷², G. Hesketh⁶³, M.D. Hildreth⁵⁵, R. Hirosky⁸¹, J.D. Hobbs⁷², B. Hoeneisen¹², H. Hoeth²⁶, M. Hohlfeld²², S.J. Hong³¹, S. Hossain⁷⁵, P. Houben³⁴, Y. Hu⁷², Z. Hubacek¹⁰, V. Hynek⁹, I. Iashvili⁶⁹, R. Illingworth⁵⁰, A.S. Ito⁵⁰, S. Jabeen⁶², M. Jaffré¹⁶, S. Jain⁷⁵, K. Jakobs²³, C. Jarvis⁶¹, R. Jesik⁴³, K. Johns⁴⁵, C. Johnson⁷⁰, M. Johnson⁵⁰, A. Jonckheere⁵⁰, P. Jonsson⁴³, A. Juste⁵⁰, E. Kajfasz¹⁵, A.M. Kalinin³⁶, J.M. Kalk⁶⁰, S. Kappler²¹, D. Karmanov³⁸, P.A. Kasper⁵⁰, I. Katsanos⁷⁰, D. Kau⁴⁹, V. Kaushik⁷⁸, R. Kehoe⁷⁹, S. Kermiche¹⁵, N. Khalatyan⁵⁰, A. Khanov⁷⁶, A. Kharchilava⁶⁹, Y.M. Khazdzhiev³⁶, D. Khatidze⁷⁰, T.J. Kim³¹, M.H. Kirby⁵³, M. Kirsch²¹, B. Klima⁵⁰, J.M. Kohli²⁷, J.-P. Konrath²³, V.M. Korablev³⁹, A.V. Kozelov³⁹, J. Kraus⁶⁵, D. Krop⁵⁴, T. Kuhl²⁴, A. Kumar⁶⁹, A. Kupco¹¹, T. Kurča²⁰, J. Kvita⁹, F. Lacroix¹³, D. Lam⁵⁵, S. Lammers⁷⁰, G. Landsberg⁷⁷, P. Lebrun²⁰, W.M. Lee⁵⁰, A. Leflat³⁸, J. Lellouch¹⁷, J. Leveque⁴⁵, J. Li⁷⁸, L. Li⁴⁸, Q.Z. Li⁵⁰, S.M. Lietti⁵, J.G.R. Lima⁵², D. Lincoln⁵⁰, J. Linnemann⁶⁵, V.V. Lipaev³⁹, R. Lipton⁵⁰, Y. Liu⁷, Z. Liu⁶, A. Lobodenko⁴⁰, M. Lokajicek¹¹, P. Love⁴², H.J. Lubatti⁸², R. Luna³, A.L. Lyon⁵⁰, A.K.A. Maciel², D. Mackin⁸⁰, R.J. Madaras⁴⁶, P. Mättig²⁶, C. Magass²¹, A. Magerkurth⁶⁴, P.K. Mal⁸², H.B. Malbouisson³, S. Malik⁶⁷, V.L. Malyshev³⁶, H.S. Mao⁵⁰, Y. Maravin⁵⁹, B. Martin¹⁴, R. McCarthy⁷², A. Melnitchouk⁶⁶, L. Mendoza⁸, P.G. Mercadante⁵, M. Merkin³⁸, K.W. Merritt⁵⁰, A. Meyer²¹, J. Meyer^{22,d}, T. Millet²⁰, J. Mitrevski⁷⁰, J. Molina³, R.K. Mommsen⁴⁴, N.K. Mondal²⁹, R.W. Moore⁶, T. Moulik⁵⁸, G.S. Muanza²⁰, M. Mulders⁵⁰, M. Mulhearn⁷⁰, O. Mundal²², L. Mundim³, E. Nagy¹⁵, M. Naimuddin⁵⁰, M. Narain⁷⁷, N.A. Naumann³⁵, H.A. Neal⁶⁴, J.P. Negret⁸, P. Neustroev⁴⁰, H. Nilsen²³, H. Nogima³, S.F. Novaes⁵, T. Nunnemann²⁵, V. O'Dell⁵⁰, D.C. O'Neil⁶, G. Obrant⁴⁰, C. Ochando¹⁶, D. Onoprienko⁵⁹, N. Oshima⁵⁰, N. Osman⁴³, J. Osta⁵⁵, R. Otec¹⁰, G.J. Otero y Garzón⁵⁰, M. Owen⁴⁴, P. Padley⁸⁰, M. Pangilinan⁷⁷, N. Parashar⁵⁶, S.-J. Park⁷¹, S.K. Park³¹,

J. Parsons⁷⁰, R. Partridge⁷⁷, N. Parua⁵⁴, A. Patwa⁷³, G. Pawloski⁸⁰, B. Penning²³, M. Perfilov³⁸, K. Peters⁴⁴,
 Y. Peters²⁶, P. Pétrouff¹⁶, M. Petteni⁴³, R. Piegaia¹, J. Piper⁶⁵, M.-A. Pleier²², P.L.M. Podesta-Lerma^{33,c},
 V.M. Podstavkov⁵⁰, Y. Pogorelov⁵⁵, M.-E. Pol², P. Polozov³⁷, B.G. Pope⁶⁵, A.V. Popov³⁹, C. Potter⁶,
 W.L. Prado da Silva³, H.B. Prosper⁴⁹, S. Protopopescu⁷³, J. Qian⁶⁴, A. Quadt^{22,d}, B. Quinn⁶⁶, A. Rakinine⁴²,
 M.S. Rangel², K. Ranjan²⁸, P.N. Ratoff⁴², P. Renkel⁷⁹, S. Reucroft⁶³, P. Rich⁴⁴, J. Rieger⁵⁴, M. Rijssenbeek⁷²,
 I. Ripp-Baudot¹⁹, F. Rizatdinova⁷⁶, S. Robinson⁴³, R.F. Rodrigues³, M. Rominsky⁷⁵, C. Royon¹⁸, P. Rubinov⁵⁰,
 R. Ruchti⁵⁵, G. Safronov³⁷, G. Sajot¹⁴, A. Sánchez-Hernández³³, M.P. Sanders¹⁷, A. Santoro³, G. Savage⁵⁰,
 L. Sawyer⁶⁰, T. Scanlon⁴³, D. Schaile²⁵, R.D. Schamberger⁷², Y. Scheglov⁴⁰, H. Schellman⁵³, T. Schliephake²⁶,
 C. Schwanenberger⁴⁴, A. Schwartzman⁶⁸, R. Schwienhorst⁶⁵, J. Sekaric⁴⁹, H. Severini⁷⁵, E. Shabalina⁵¹,
 M. Shamim⁵⁹, V. Shary¹⁸, A.A. Shchukin³⁹, R.K. Shivpuri²⁸, V. Siccaldi¹⁹, V. Simak¹⁰, V. Sirotenko⁵⁰, P. Skubic⁷⁵,
 P. Slattery⁷¹, D. Smirnov⁵⁵, G.R. Snow⁶⁷, J. Snow⁷⁴, S. Snyder⁷³, S. Söldner-Rembold⁴⁴, L. Sonnenschein¹⁷,
 A. Sopczak⁴², M. Sosebee⁷⁸, K. Soustruznik⁹, B. Spurlock⁷⁸, J. Stark¹⁴, J. Steele⁶⁰, V. Stolin³⁷, D.A. Stoyanova³⁹,
 J. Strandberg⁶⁴, S. Strandberg⁴¹, M.A. Strang⁶⁹, E. Strauss⁷², M. Strauss⁷⁵, R. Ströhmer²⁵, D. Strom⁵³,
 L. Stutte⁵⁰, S. Sumowidagdo⁴⁹, P. Svoisky⁵⁵, A. Sznajder³, P. Tamburello⁴⁵, A. Tanasijczuk¹, W. Taylor⁶,
 J. Temple⁴⁵, B. Tiller²⁵, F. Tissandier¹³, M. Titov¹⁸, V.V. Tokmenin³⁶, T. Toole⁶¹, I. Torchiani²³, T. Trefzger²⁴,
 D. Tsybychev⁷², B. Tuchming¹⁸, C. Tully⁶⁸, P.M. Tuts⁷⁰, R. Unalan⁶⁵, L. Uvarov⁴⁰, S. Uvarov⁴⁰, S. Uzunyan⁵²,
 B. Vachon⁶, P.J. van den Berg³⁴, R. Van Kooten⁵⁴, W.M. van Leeuwen³⁴, N. Varelas⁵¹, E.W. Varnes⁴⁵,
 I.A. Vasilyev³⁹, M. Vaupel²⁶, P. Verdier²⁰, L.S. Vertogradov³⁶, M. Verzocchi⁵⁰, F. Villeneuve-Seguié⁴³, P. Vint⁴³,
 P. Vokac¹⁰, E. Von Toerne⁵⁹, M. Voutilainen^{68,e}, R. Wagner⁶⁸, H.D. Wahl⁴⁹, L. Wang⁶¹, M.H.L.S. Wang⁵⁰,
 J. Warchol⁵⁵, G. Watts⁸², M. Wayne⁵⁵, G. Weber²⁴, M. Weber⁵⁰, L. Welty-Rieger⁵⁴, A. Wenger^{23,f},
 N. Wermes²², M. Wetstein⁶¹, A. White⁷⁸, D. Wicke²⁶, G.W. Wilson⁵⁸, S.J. Wimpenny⁴⁸, M. Wobisch⁶⁰,
 D.R. Wood⁶³, T.R. Wyatt⁴⁴, Y. Xie⁷⁷, S. Yacoob⁵³, R. Yamada⁵⁰, M. Yan⁶¹, T. Yasuda⁵⁰, Y.A. Yatsunenkov³⁶,
 K. Yip⁷³, H.D. Yoo⁷⁷, S.W. Youn⁵³, J. Yu⁷⁸, A. Zatserklyaniy⁵², C. Zeitnitz²⁶, T. Zhao⁸², B. Zhou⁶⁴,
 J. Zhu⁷², M. Zielinski⁷¹, D. Zieminska⁵⁴, A. Zieminski^{54,‡}, L. Zivkovic⁷⁰, V. Zutshi⁵², and E.G. Zverev³⁸

(The DØ Collaboration)

¹Universidad de Buenos Aires, Buenos Aires, Argentina

²LAFEX, Centro Brasileiro de Pesquisas Físicas, Rio de Janeiro, Brazil

³Universidade do Estado do Rio de Janeiro, Rio de Janeiro, Brazil

⁴Universidade Federal do ABC, Santo André, Brazil

⁵Instituto de Física Teórica, Universidade Estadual Paulista, São Paulo, Brazil

⁶University of Alberta, Edmonton, Alberta, Canada,

Simon Fraser University, Burnaby, British Columbia,

Canada, York University, Toronto, Ontario, Canada,

and McGill University, Montreal, Quebec, Canada

⁷University of Science and Technology of China, Hefei, People's Republic of China

⁸Universidad de los Andes, Bogotá, Colombia

⁹Center for Particle Physics, Charles University, Prague, Czech Republic

¹⁰Czech Technical University, Prague, Czech Republic

¹¹Center for Particle Physics, Institute of Physics,
Academy of Sciences of the Czech Republic, Prague, Czech Republic

¹²Universidad San Francisco de Quito, Quito, Ecuador

¹³LPC, Univ Blaise Pascal, CNRS/IN2P3, Clermont, France

¹⁴LPSC, Université Joseph Fourier Grenoble 1, CNRS/IN2P3,

Institut National Polytechnique de Grenoble, France

¹⁵CPPM, IN2P3/CNRS, Université de la Méditerranée, Marseille, France

¹⁶LAL, Univ Paris-Sud, IN2P3/CNRS, Orsay, France

¹⁷LPNHE, IN2P3/CNRS, Universités Paris VI and VII, Paris, France

¹⁸DAPNIA/Service de Physique des Particules, CEA, Saclay, France

¹⁹IPHC, Université Louis Pasteur et Université de Haute Alsace, CNRS/IN2P3, Strasbourg, France

²⁰IPNL, Université Lyon 1, CNRS/IN2P3, Villeurbanne, France and Université de Lyon, Lyon, France

²¹III. Physikalisches Institut A, RWTH Aachen, Aachen, Germany

²²Physikalisches Institut, Universität Bonn, Bonn, Germany

²³Physikalisches Institut, Universität Freiburg, Freiburg, Germany

²⁴Institut für Physik, Universität Mainz, Mainz, Germany

²⁵Ludwig-Maximilians-Universität München, München, Germany

²⁶Fachbereich Physik, University of Wuppertal, Wuppertal, Germany

²⁷Panjab University, Chandigarh, India

- ²⁸Delhi University, Delhi, India
- ²⁹Tata Institute of Fundamental Research, Mumbai, India
- ³⁰University College Dublin, Dublin, Ireland
- ³¹Korea Detector Laboratory, Korea University, Seoul, Korea
- ³²SungKyunKwan University, Suwon, Korea
- ³³CINVESTAV, Mexico City, Mexico
- ³⁴FOM-Institute NIKHEF and University of Amsterdam/NIKHEF, Amsterdam, The Netherlands
- ³⁵Radboud University Nijmegen/NIKHEF, Nijmegen, The Netherlands
- ³⁶Joint Institute for Nuclear Research, Dubna, Russia
- ³⁷Institute for Theoretical and Experimental Physics, Moscow, Russia
- ³⁸Moscow State University, Moscow, Russia
- ³⁹Institute for High Energy Physics, Protvino, Russia
- ⁴⁰Petersburg Nuclear Physics Institute, St. Petersburg, Russia
- ⁴¹Lund University, Lund, Sweden, Royal Institute of Technology and Stockholm University, Stockholm, Sweden, and Uppsala University, Uppsala, Sweden
- ⁴²Lancaster University, Lancaster, United Kingdom
- ⁴³Imperial College, London, United Kingdom
- ⁴⁴University of Manchester, Manchester, United Kingdom
- ⁴⁵University of Arizona, Tucson, Arizona 85721, USA
- ⁴⁶Lawrence Berkeley National Laboratory and University of California, Berkeley, California 94720, USA
- ⁴⁷California State University, Fresno, California 93740, USA
- ⁴⁸University of California, Riverside, California 92521, USA
- ⁴⁹Florida State University, Tallahassee, Florida 32306, USA
- ⁵⁰Fermi National Accelerator Laboratory, Batavia, Illinois 60510, USA
- ⁵¹University of Illinois at Chicago, Chicago, Illinois 60607, USA
- ⁵²Northern Illinois University, DeKalb, Illinois 60115, USA
- ⁵³Northwestern University, Evanston, Illinois 60208, USA
- ⁵⁴Indiana University, Bloomington, Indiana 47405, USA
- ⁵⁵University of Notre Dame, Notre Dame, Indiana 46556, USA
- ⁵⁶Purdue University Calumet, Hammond, Indiana 46323, USA
- ⁵⁷Iowa State University, Ames, Iowa 50011, USA
- ⁵⁸University of Kansas, Lawrence, Kansas 66045, USA
- ⁵⁹Kansas State University, Manhattan, Kansas 66506, USA
- ⁶⁰Louisiana Tech University, Ruston, Louisiana 71272, USA
- ⁶¹University of Maryland, College Park, Maryland 20742, USA
- ⁶²Boston University, Boston, Massachusetts 02215, USA
- ⁶³Northeastern University, Boston, Massachusetts 02115, USA
- ⁶⁴University of Michigan, Ann Arbor, Michigan 48109, USA
- ⁶⁵Michigan State University, East Lansing, Michigan 48824, USA
- ⁶⁶University of Mississippi, University, Mississippi 38677, USA
- ⁶⁷University of Nebraska, Lincoln, Nebraska 68588, USA
- ⁶⁸Princeton University, Princeton, New Jersey 08544, USA
- ⁶⁹State University of New York, Buffalo, New York 14260, USA
- ⁷⁰Columbia University, New York, New York 10027, USA
- ⁷¹University of Rochester, Rochester, New York 14627, USA
- ⁷²State University of New York, Stony Brook, New York 11794, USA
- ⁷³Brookhaven National Laboratory, Upton, New York 11973, USA
- ⁷⁴Langston University, Langston, Oklahoma 73050, USA
- ⁷⁵University of Oklahoma, Norman, Oklahoma 73019, USA
- ⁷⁶Oklahoma State University, Stillwater, Oklahoma 74078, USA
- ⁷⁷Brown University, Providence, Rhode Island 02912, USA
- ⁷⁸University of Texas, Arlington, Texas 76019, USA
- ⁷⁹Southern Methodist University, Dallas, Texas 75275, USA
- ⁸⁰Rice University, Houston, Texas 77005, USA
- ⁸¹University of Virginia, Charlottesville, Virginia 22901, USA and
- ⁸²University of Washington, Seattle, Washington 98195, USA

(Dated: March 11, 2008)

We report the results of a search for pair production of doubly-charged Higgs bosons via $p\bar{p} \rightarrow H^{++}H^{--}X \rightarrow \mu^+\mu^+\mu^-\mu^-X$ at $\sqrt{s} = 1.96$ TeV. We use a dataset corresponding to an integrated luminosity of 1.1 fb^{-1} collected from 2002 to 2006 by the D0 detector at the Fermilab Tevatron Collider. In the absence of an excess above the standard model background, lower mass limits of $M(H_L^{\pm\pm}) > 150 \text{ GeV}/c^2$ and $M(H_R^{\pm\pm}) > 127 \text{ GeV}/c^2$ at 95% C.L. are set, respectively, for left-handed and right-handed doubly-charged Higgs bosons assuming a 100% branching ratio into muons.

In the standard model (SM) of electroweak interactions, elementary fermions and bosons acquire mass via a weak isospin scalar doublet. This mechanism results in the existence of an additional particle, the Higgs boson, which has not yet been observed. Extensions of the Higgs sector involving higher isospin multiplets predict the existence of doubly-charged Higgs bosons which can be relatively light and hence accessible at current experimental facilities. Doubly-charged Higgs bosons appear in many scenarios such as left-right symmetric models [1], Higgs triplet models [2], and Little Higgs models [3]. At the Fermilab Tevatron Collider, the two main production mechanisms are pair production via $p\bar{p} \rightarrow Z/\gamma^* X \rightarrow H^{++}H^{--}X$ and single production via WW fusion, $p\bar{p} \rightarrow W^\pm W^\pm X \rightarrow H^{\pm\pm}X$. However, higher isospin Higgs multiplets are generally severely constrained by $\rho \equiv m_W^2/(\cos\theta_W m_Z)^2 = 1$ at tree level. The existing phenomenological and theoretical constraints are easily satisfied when the $W^\pm W^\pm \rightarrow H^{\pm\pm}$ coupling is vanishing [4]. If the H^{++} coupling to W boson pairs is suppressed, the dominant final states are expected to be like-sign lepton pairs. Left-handed ($H_L^{\pm\pm}$) and right-handed ($H_R^{\pm\pm}$) states are distinguished by their coupling to left-handed and right-handed leptons, respectively. The pair production cross section for left-handed doubly-charged Higgs bosons for $100 \leq M(H^{\pm\pm}) \leq 200$ GeV/ c^2 is about a factor two larger than that for the right-handed states due to different couplings to the intermediate Z boson [5]. Previous searches for $H^{\pm\pm}$ have been performed by the LEP collaborations [6] in e^+e^- collisions and by the D0 [7] and CDF [8] collaborations at the Tevatron $p\bar{p}$ collider. This Letter presents the results of a direct search for $p\bar{p} \rightarrow H^{++}H^{--}X$ with $H^{\pm\pm} \rightarrow \mu^\pm\mu^\pm$ by the D0 collaboration with improved sensitivity.

The main D0 detector systems are a central tracking system, a liquid-argon and uranium calorimeter, and a muon detector [9]. The central tracking system consists of the silicon microstrip tracker (SMT) and the central fiber tracker (CFT) surrounded by a 2 T solenoidal magnet, with designs optimized for tracking and vertexing capability at pseudorapidity [10] $|\eta| < 3$ and $|\eta| < 2.5$, respectively. The liquid-argon and uranium calorimeter has a central calorimeter (CC) covering a region up to $|\eta| \approx 1.1$ and two end calorimeters (EC) extending the coverage to $|\eta| \approx 4.2$, with each housed in a separate cryostat [11]. The muon detector has layers of proportional drift tubes and scintillation counters before and after a 1.8 T iron toroid [12]. This analysis is based on the Run II data set collected with the D0 detector at the Fermilab Tevatron Collider at $\sqrt{s} = 1.96$ TeV from April 2002 to February 2006 corresponding to 1.1 fb $^{-1}$. Events are collected using a suite of dimuon and single muon triggers.

In the previous D0 analysis [7], two like-sign muons were required in the final state. In this analysis, we require a third muon, which increases the sensitivity by decreasing backgrounds. We follow five steps to select events. In the first step (S1), events are required to have at least two muons. Each muon must have a transverse momentum $p_T > 15$ GeV/ c and $|\eta| < 2.0$. Muons are selected using patterns of hits in the wire chambers and scintillators in the muon system. Each muon must be matched to a track in the central tracker with at least five hits in the CFT layers and at least two hits in the SMT layers. Muons from cosmic rays are removed by using a timing information on the hits in the scintillator layers.

In the second step (S2), isolation criteria based on the calorimeter and tracking information are applied to remove the background from multijet production with muons originating from in-flight decay of pions or kaons, or from semi-leptonic decays of B or D mesons. The sum of the transverse energies of the calorimeter cells in an annulus of radius $0.1 < \mathcal{R} < 0.4$, where $\mathcal{R} = \sqrt{(\Delta\phi)^2 + (\Delta\eta)^2}$ and ϕ is the azimuthal angle, around the muon direction is required to be less than 2.5 GeV. A similar condition is defined for the scalar sum of the p_T of all tracks, excluding the muon in a cone of radius $\mathcal{R} = 0.5$ centered around the muon, which must be less than 2.5 GeV/ c .

Selection S3 reduces the remaining $Z \rightarrow \mu^+\mu^-$ and multijet backgrounds. The azimuthal angle $\Delta\phi$ between at least one pair of muons is required to be less than 2.5 radians, since the two muons from Z boson decays are mostly back-to-back. This requirement also rejects a fraction of the multijet background with nearly back-to-back muons.

Selection S4 requires at least two muons to be of like sign. The final selection (S5) requires a third muon, satisfying the S1 selection and the isolation selection criteria S2 but without the minimum hit requirement on the central track.

The dominant background in this analysis arises from electroweak processes where real high p_T muons are created from W or Z boson decays as well as non-isolated muons originating from jets. The SM backgrounds and signal processes are generated with PYTHIA [13] and normalized using the theoretical cross section. The $Z/\gamma^* \rightarrow \ell^+\ell^-$ cross section is calculated at next-to-next-to-leading order (NNLO) [14]. The $t\bar{t}$ cross section is calculated at NNLO [15] and the WW , ZZ and WZ cross sections are calculated with MCFM [16] at next-to-leading order (NLO). All samples are processed through the D0 detector simulation based on GEANT [17] and the same reconstruction software as for the data. The muon reconstruction and isolation efficiencies differ between Monte

TABLE I: The expected numbers of events for a signal with $M(H_L^{\pm\pm}) = 140 \text{ GeV}/c^2$ and background and the number of observed events after each selection step. The statistical and systematical uncertainties are combined in the table.

Selection	Preselection	Isolation	$\Delta\phi < 2.5$	Like sign	Third muon
	S1	S2	S3	S4	S5
$Z/\gamma^* \rightarrow \mu^+\mu^-$	69181 ± 4642	58264 ± 3910	4936 ± 333	5.3 ± 1.6	< 0.01
Multijet	4492 ± 120	194 ± 18	18 ± 2	6.3 ± 0.8	0.2 ± 0.1
$Z/\gamma^* \rightarrow \tau^+\tau^-$	328 ± 25	269 ± 21	20 ± 3	< 0.01	< 0.01
$t\bar{t}$	38 ± 3	20 ± 1	14 ± 1	0.03 ± 0.01	< 0.01
WW	40 ± 3	34 ± 2	20 ± 1	< 0.01	< 0.01
WZ	19 ± 1	16 ± 1	11 ± 1	2.95 ± 0.20	1.62 ± 0.11
ZZ	10 ± 1	9 ± 1	5 ± 1	0.63 ± 0.05	0.47 ± 0.03
Total background	74108 ± 4644	58806 ± 3910	5024 ± 333	15.2 ± 1.8	2.3 ± 0.2
Signal	20.5 ± 2.7	18.5 ± 2.4	16.3 ± 2.1	11.6 ± 1.5	10.1 ± 1.3
Data	72974	58763	4558	16	3

Carlo (MC) and data, and these differences are corrected. Trigger efficiency corrections are not applied to the MC sample. Instead, the MC sample are normalized to the data using the Z boson mass peak at the selection level S2.

Another important background comes from multijet production, mainly $b\bar{b}$ events decaying semi-leptonically into muons that appear isolated. The multijet background is derived from the data sample with non-isolated muons obtained by inverting the isolation requirements for both muons after the selection S1. The efficiency of the isolation requirement is assumed to be identical for multijet events with like-sign and opposite-sign muon pairs. It is also assumed that all like-sign events after subtracting SM backgrounds are multijet events. The SM backgrounds are subtracted in the following samples used for the multijet background determination. The total number of multijet events before the isolation requirement (4492 ± 120) is then given by the number of non-isolated events for all charge combinations multiplied by the ratio of the total number of events to the number of non-isolated events in the like-sign sample. The number of multijet events after the isolation requirement (194 ± 18) is obtained by multiplying this number with the isolation efficiency ($4.3 \pm 0.5\%$), given by the ratio of isolated to all like-sign multijet events.

A second instrumental background arises from $Z/\gamma^* \rightarrow \mu^+\mu^-$ events in which the charge of one of the muons is misidentified. The first source of charge misidentification is due to fewer CFT layers at large η and a consequent increase in the charge misidentification probability. The second source affects very high p_T tracks for which the uncertainty on the measured curvature can cause charge misidentification. The charge misidentification rate is obtained by dividing the number of like-sign events (S1, S2 and S4) by the number of events without the like-sign requirement (S1 and S2) in the dimuon invariant mass region above $70 \text{ GeV}/c^2$, after subtracting the SM sources of background except $Z/\gamma^* \rightarrow \mu^+\mu^-$

events from the data. This mass requirement removes most multijet background events in the low mass range. From these ratios, we determine the average probability for charge misidentification in data and MC to be $P_{\text{data}} = (6.2 \pm 1.1) \times 10^{-4}$ and $P_{\text{MC}} = (3.1 \pm 0.4) \times 10^{-4}$, respectively, assuming the multijet background is negligible. The uncertainties are statistical. Since the charge misidentification rate in MC is underestimated, the ratio of P_{data} to P_{MC} is taken as a correction equal to 2.0 ± 0.4 . This ratio is applied to the $Z/\gamma^* \rightarrow \mu^+\mu^-$ MC sample when estimating the like-sign contribution.

The distributions of dimuon invariant mass and $\Delta\phi$ after the selection S1 are shown in Fig. 1 (a) and (b). The data are compared with the sum of the background contributions. For those events with more than one pair of muons fulfilling the selection criteria, the dimuon invariant mass and $\Delta\phi$ are calculated only for the pair with the highest individual momenta. The numbers of remaining events after each selection are shown in Table I. There is good agreement between data and the sum of the backgrounds. Figure 1 (c) and (d) show the

TABLE II: The numbers of observed and expected background events after each selection criterion with the like-sign requirement applied together with S1. The statistical and systematical uncertainties are combined in the table.

Selection (Like-sign)	Preselection	Isolation	$\Delta\phi < 2.5$
	S1 & S4	S2	S3
$Z/\gamma^* \rightarrow \mu^+\mu^-$	84 ± 24	42 ± 12	5.3 ± 1.6
Multijet	1620 ± 34	70 ± 5	6.3 ± 0.8
$Z/\gamma^* \rightarrow \tau^+\tau^-$	3.2 ± 1.3	0.2 ± 0.3	< 0.01
$t\bar{t}$	6.6 ± 0.5	< 0.1	< 0.1
WW	0.08 ± 0.02	0.04 ± 0.01	< 0.01
WZ	5.14 ± 0.35	4.25 ± 0.29	2.95 ± 0.20
ZZ	1.12 ± 0.08	0.90 ± 0.06	0.63 ± 0.05
Total background	1720 ± 41	117 ± 13	15.2 ± 1.8
Data	1678	96	16

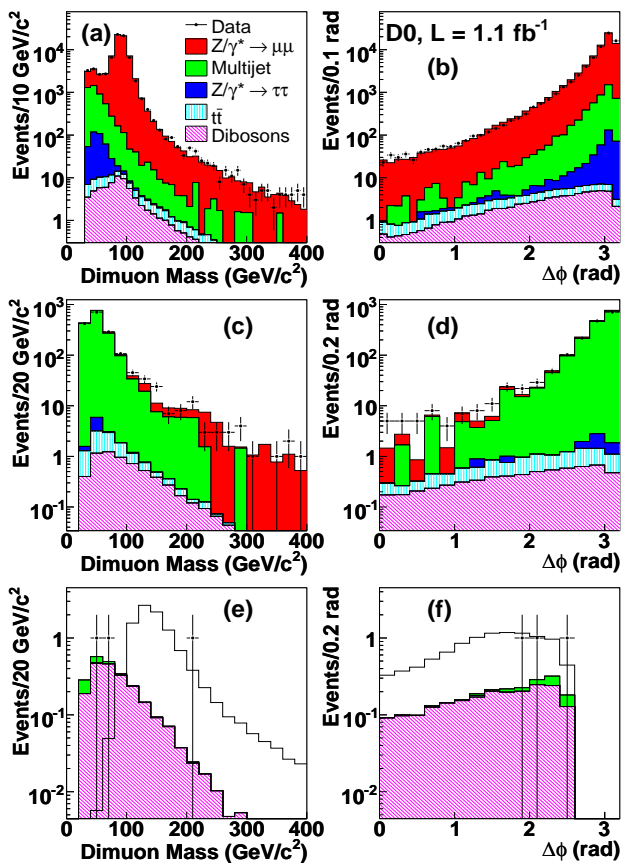


FIG. 1: Distributions of the dimuon invariant mass and $\Delta\phi$ between the two muons for data compared to the sum of MC backgrounds after the selection S1 (a, b), the preselection S1 with the like-sign requirement S4 (c, d) and the final requirement S1–S5 (e, f). The signal expected for a left-handed $H^{\pm\pm}$, with $M(H^{\pm\pm}) = 140 \text{ GeV}/c^2$, is also shown by the open histogram (e, f).

dimuon invariant mass and $\Delta\phi$ distributions after the S1 and S4 requirements. The excess of events at $150 \text{ GeV}/c^2$ has a significance of less than 2.6σ . Table II gives the individual like-sign backgrounds after the various selection stages. This demonstrates that the like-sign backgrounds are well understood.

After all five selection criteria, three data events remain, in good agreement with the SM background expectation of 2.3 ± 0.2 events. Total signal efficiencies are 32%–34% and are nearly independent of mass. The dimuon invariant mass and $\Delta\phi$ distributions for these events are compared to the sum of the backgrounds in Fig. 1 (e) and (f).

Since no excess is observed, we use the dimuon invariant mass distribution in Fig. 1 (e) to compute upper limits on the production cross section times branching fraction as a function of $M(H^{\pm\pm})$ using the CL_S method [18] as implemented in the MCLIMIT program [19]. The expected rate for the signal as a function of $M(H^{\pm\pm})$ is determined by the next-to-leading order (NLO) cross sec-

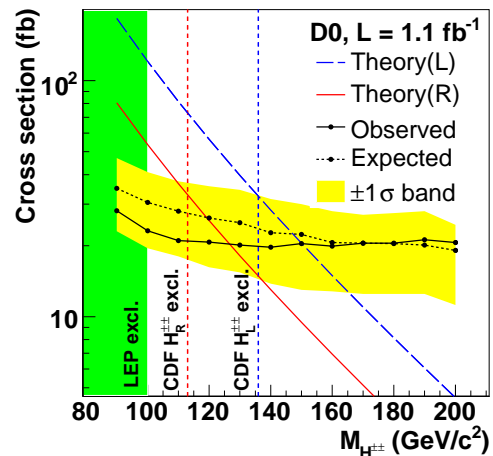


FIG. 2: The cross section limit as a function of the Higgs mass $M(H^{\pm\pm})$ at the 95% C.L. The mass regions excluded by LEP and CDF are also shown. The $\pm 1\sigma$ uncertainty on the expected limit is given by the yellow band (color online).

tion [5] and measured luminosity, corrected for the signal efficiency.

A number of systematic uncertainties on signal and background are taken into account in the limit calculation. The uncertainties on the correction of the muon identification are 2% and 6% for backgrounds and signal, respectively. The uncertainty on the isolation efficiency for the multijet background is 12%. The 20% uncertainty on the correction for charge misidentification is included. The uncertainty on the luminosity for signal is estimated to be 6.1% [20]. The uncertainty on the normalization using NNLO MC SM background production cross sections is taken to be 5%. The PDF uncertainties on the cross section for backgrounds are taken to be 4% [21].

The cross section limit as a function of $M(H^{\pm\pm})$ is shown in Fig. 2 together with the theoretical cross section for left- and right-handed doubly charged Higgs bosons. At the 95% C.L., lower mass limits of $150 \text{ GeV}/c^2$ for left-handed and $127 \text{ GeV}/c^2$ for right-handed doubly-charged Higgs bosons are obtained. This significantly extends the previous mass limit [8] for a doubly-charged Higgs boson decaying into muons.

We thank the staffs at Fermilab and collaborating institutions, and acknowledge support from the DOE and NSF (USA); CEA and CNRS/IN2P3 (France); FASI, Rosatom and RFBR (Russia); CNPq, FAPERJ, FAPESP and FUNDUNESP (Brazil); DAE and DST (India); Colciencias (Colombia); CONACyT (Mexico); KRF and KOSEF (Korea); CONICET and UBACyT (Argentina); FOM (The Netherlands); STFC (United Kingdom); MSMT and GACR (Czech Republic); CRC Program, CFI, NSERC and WestGrid Project (Canada); BMBF and DFG (Germany); SFI (Ireland); The Swedish Research Council (Sweden); CAS and CNSF (China); and the Alexander von Humboldt Foundation.

-
- [a] Visitor from Augustana College, Sioux Falls, SD, USA.
- [b] Visitor from The University of Liverpool, Liverpool, UK.
- [c] Visitor from ICN-UNAM, Mexico City, Mexico.
- [d] Visitor from II. Physikalisches Institut, Georg-August-University, Göttingen, Germany.
- [e] Visitor from Helsinki Institute of Physics, Helsinki, Finland.
- [f] Visitor from Universität Zürich, Zürich, Switzerland.
- [‡] Deceased.
- [1] J.C. Pati and A. Salam, *Phys. Rev. D* **10**, 275 (1974); R.N. Mohapatra and J.C. Pati, *Phys. Rev. D* **11**, 566 (1975); R.N. Mohapatra and J.C. Pati, *Phys. Rev. D* **11**, 2558 (1975); G. Senjanovic and R.N. Mohapatra, *Phys. Rev. D* **12**, 1502 (1975).
- [2] G.B. Gelmini and M. Roncadelli, *Phys. Lett. B* **99**, 411 (1981).
- [3] N. Arkani-Hamed, A.G. Cohen and H. Georgi, *Phys. Lett. B* **513**, 232 (2001).
- [4] J.F. Gunion, H.E. Haber, G. Kane and S. Dawson, *The Higgs Hunter's Guide* (Frontiers in Physics, Addison-Wesley, Redwood City, CA, 1989).
- [5] M. Mühlleitner and M. Spira, *Phys. Rev. D* **68**, 117701 (2003).
- [6] OPAL Collaboration, G. Abbiendi *et al.*, *Phys. Lett. B* **526**, 221 (2002); OPAL Collaboration, P.D. Acton *et al.*, *Phys. Lett. B* **295**, 347 (1992); L3 Collaboration, P. Achard *et al.*, *Phys. Lett. B* **576**, 18 (2003); DELPHI Collaboration, J. Abdallah *et al.*, *Phys. Lett. B* **552**, 127 (2003).
- [7] D0 Collaboration, V.M. Abazov *et al.*, *Phys. Rev. Lett.* **93**, 141801 (2004).
- [8] CDF Collaboration, D. Acosta *et al.*, *Phys. Rev. Lett.* **93**, 221802 (2004).
- [9] D0 Collaboration, V.M. Abazov *et al.*, *Nucl. Instrum. Methods in Phys. Res. A* **565**, 463 (2006).
- [10] The pseudorapidity is defined as $\eta = -\ln \left[\tan \left(\frac{\theta}{2} \right) \right]$ as a function of the polar angle θ .
- [11] D0 Collaboration, S. Abachi *et al.*, *Nucl. Instrum. Methods in Phys. Res. A* **338**, 185 (1994).
- [12] V.M. Abazov *et al.*, *Nucl. Instrum. Methods in Phys. Res. A* **552**, 372 (2005).
- [13] T. Sjöstrand *et al.*, *Comput. Phys. Commun.* **135**, 238 (2001).
- [14] R. Hamberg, W.L. van Neerven and T. Matsuura, *Nucl. Phys.* **B359**, 343 (1991) [Erratum-*ibid.* **B644**, 403 (2002)].
- [15] N. Kidonakis and R. Vogt, *Int. J. Mod. Phys. A* **20**, 3171 (2005).
- [16] J.M. Campbell and R.K. Ellis, *Phys. Rev. D* **60**, 113006 (1999), <http://mcfm.fnal.gov/>.
- [17] R. Brun and F. Carminati, CERN Program Library Long Writeup W5013 (1993).
- [18] A. Read, *J. Phys. G: Nucl. Part. Phys.* **28**, 2693 (2002).
- [19] T. Junk, *Nucl. Instrum. Methods in Phys. Res. A* **434**, 435 (1999).
- [20] T. Andeen *et al.*, FERMILAB-TM-2365 (2007).
- [21] J. Pumplin *et al.*, *J. High Energy Phys.* **07**, 12 (2002).